Project Title: Finite Element Solution of Thermal Gee-Lyon Flows in a Circular Tube

Student: Narken Aimambet
Advisor: Prof. Dongming Wei
Second reader: Prof. Yogi Erlangga

Department of Mathematics, Nazarbayev University, Astana, Kazakhstan
May, 2016

Abstract: The goal of this project is to calculate the temperature distribution of certain pressure-driven non-Newtonian flows inside a circular tube. The rheology under consideration is the type in which the shear stress is an implicit function of the shear rate defined as the inverse function of an odd function. The fluid velocity in the tube is approximated by the steady state velocity profile along the tube length and the viscosity is assumed to be independent of the temperature. The velocity profile is computed by using Mathematica's build-in ODE solver semi-analytically. The corresponding steady state temperature profile at tube length is then calculated taking into account of heat source generated by shear rate from the fluid flow by solving an ODE. The temperature distribution from the entrance to the fully developed region is then approximated numerically by using the axisymmetric linear triangular finite elements. Material and geometric constants and data for extrusion of chemical Lucite through the tube in literature are used for the numerical example. Comparison of the numerical result with the industrial experimental result is made at a point along the central axis of the tube.

Key words: Non-Newtonian fluid, finite element method, temperature distribution, extrusion

1 Introduction

In numerous manufacturing processes viscous non-Newtonian fluids are forced through channels which are often at a temperature different from that of the fluid. Determining the temperature distribution to the non-isothermal laminar flows for these viscous fluids in the channels can be very difficult due to boundary layers near the fluid entrance region and the coupling of fluid velocity with viscosity and temperature as well as convective diffusion. The limitations to applying conventional methods used for Newtonian flows to the problem of non-isothermal flow of viscous non-Newtonian fluids are:

- The viscosity of most viscous fluids changes with temperature and therefore heat transfer affects the velocity distribution
- Fluid viscosity changes with shear stress
- Frictional heat generated during the flow and cooling due to shear stress of the fluids
- Variations of thermal diffusivity and heat capacity with temperature

The experiment of extrusion of the flows in the channels from which the mathematical model is derived was carried out by the following method: The fluid is forced through a tube of circular cross section, in which the wall temperature is constant but may be different from that of the initial fluid temperature. The fluid enters the tube at all times at a uniform constant temperature, T_0. The solution of the problem starts with the tube full of fluid at temperature T_0. At time zero, a pressure, P_0, is applied at the inlet of the tube to create a constant pressure gradient, and simultaneously the wall temperature T_w , is changed to a desired value. The applied pressure and wall temperature are held constant in this experiment.

As a fluid flows inside the tube, the rate of shear stress that it undergoes depends on the shear strain. This means that the change in velocity with respect to distance from the boundary is a function of shearing force. Newton proposed that shear rate is directly proportional to the shear stress, with proportionality constant called viscosity, denoted by η. It was initially thought that viscosity was a true constant for any liquid at constant temperature. For steady state Newtonian flows in circular tubes, we have

$$\tau = -\eta \frac{du}{dr}, \tag{1}$$

where τ is the shear stress, $\frac{du}{dr}$ the corresponding shear strain, and r the radial coordinate.

Many viscous fluids like plastic melts do not follow this linear law and, as a result, these fluids are called "non-Newtonian". For instance, for the non-Newtonian Gee-Lyon fluid flows, the following rheology equation is considered to be in a good fit with the experimental data for Lucite:

$$\frac{du}{dr} = -C\tau(1 + k|\tau|^n), \tag{2}$$

where C is a temperature-dependent parameter, and k and n are characteristic constants for a particular fluid that are temperature independent; see (Gee & Lyon,1956) for details.

In this report, we will consider numerical simulations of extrusions of thermal fluid flows in a circular tube governed by the rheology equation (2). In particular, we will focus on extrusion of Lucite through a channel with a diameter D, with material properties taken from Gee and Lyon, 1956. Figure 1 shows the behavior of viscosity and shear stress of Lucite, where shear stress was derived from equation (2). We note that for Lucite $n = 2$. First, the function of the velocity is going to be found based on the given conditions, and the properties of Lucite (Gee & Lyon1956). Second, the fully developed temperature along the tube-length will be computed by using finite elements. We will compare how it matches with the results found in Gee and Lyon's paper. Finally, using the finite element method we will find the temperature distribution in the tube where temperature is not fully developed. The accuracy of results obtained by the above described method can be justified mathematically by the theory developed by Wei, D. Zhang, Z. (2001).

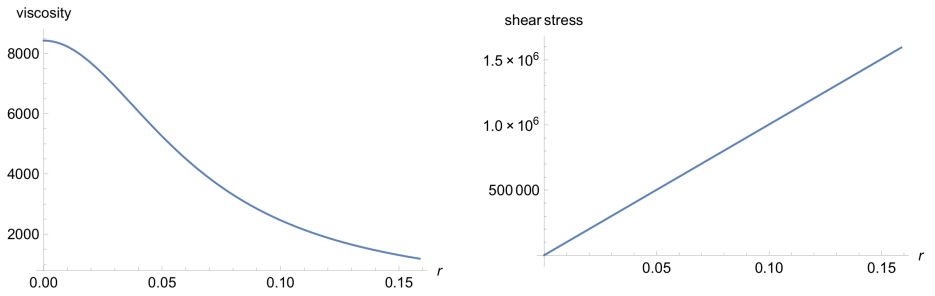

(a) Viscosity

(b) Shear Stress

Figure 1: Pictures of viscosity and shear stress

For results of this problem based on a similar non-Newtonian fluid flow, see Agur, E.E. Vlachopoulos, J. (1981) and Wei, D. Luo, H. (2003).

2 The heat equation

The temperature distribution of a fluid flowing axisymmetrically inside a circular channel can be modeled by the heat equation (in the Polar coordinate)

$$\rho C_p u \frac{\partial T}{\partial z} = \kappa\left(\frac{\partial^2 T}{\partial r^2} + \frac{1}{r}\frac{\partial T}{\partial r} + \frac{\partial^2 T}{\partial z^2}\right) + \tau\frac{du}{dr}, \tag{3}$$

where $T = T(r, z)$ is the temperature of the fluid at the point (r, z) (see Figure 2), ρ the density, C_p the heat capacity, κ the conductivity, and $u = u(r, z)$ the fluid velocity. The term $\tau\frac{du}{dr}$ represents the heat generated by the viscous shearing of the fluid in the tube, which in this paper is modeled by the rheology equation (2). For this rheology equation, τ is determined from the relation

$$\tau = \frac{r}{2L_0}\frac{dP}{dz}, \tag{4}$$

where L_0 is the length of the tube. By combining (4) and (2) the term $\tau\frac{du}{dr}$ is known for a given $\frac{dP}{dz}$.

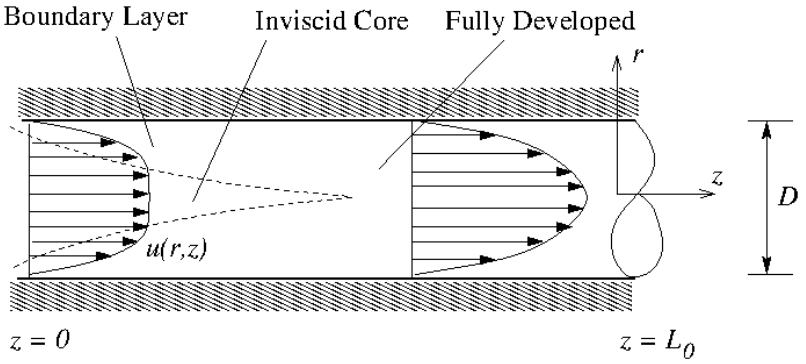

Figure 2: Behavior of fluid inside the tube

Equation (3) can in principle be solved if a set of boundary conditions is imposed. To mimic the extrusion process we impose the following conditions:

$$\begin{aligned} &\text{at } r = \frac{D}{2} = R_0, \qquad T(R_0, z) = T_w, \\ &\text{at } z = 0, \qquad\qquad\quad T(r, 0) = T_0. \end{aligned} \tag{5}$$

In this paper we solve (3) with boundary conditions (5) by a finite element method.

In the subsequent section, we shell discuss some dynamics of fluid flowing in a channel, which are relevant to our modeling problem.

2.1 Fully Developed Velocity Distribution

In order to solve (3) we need to know the velocity distribution of the fluid. Ideally the velocity distribution has to be determined from the incompressible Navier-Stokes equations. This leads to a coupled system of equations, which requires a simultaneous solutions of (3) and the Navier-Stokes equations. In our case, however, we assume that velocity distributions at any location z is the same as that in the fully developed region. This assumption certainly does not hold in the entrance region we are interested in. We however expect that the velocity distribution from the fully developed region does not differ too much from those in the entrance region, and hence can serve as a good approximation. In the fully developed region the velocity distribution for Lucite ($n = 2$) is given by

$$\frac{du}{dr} = -C\tau(1 + k|\tau|^2) = -\frac{C}{2L_0}\frac{dP}{dz}r - \frac{kC}{8L_0^3}\left(\frac{dP}{dz}\right)^3 r^3, \tag{6}$$

with boundary conditions $u(R_0) = 0$ and $\frac{du}{dr}(0) = 0$. Note that the second condition is automatically satisfied, so we just need the first condition to determine uniquely the fully developed velocity distribution. The solution of (6) is given by the following:

$$u(r) = -\frac{1}{4}C\frac{1}{L_0}\frac{dP}{dz}(r^2 - R_0^2) - \frac{1}{32}Ck\big(\frac{1}{L_0}\frac{dP}{dz}\big)^3(r^4 - R_0^4).$$

Figure 3 shows the fully developed velocity distribution for Lucite with the following experimental conditions:

- $C = 1.187 \times 10^{-4}$
- $k = 2.4 \times 10^{-12}$ cm^2/dyne^2
- $L_0 = 10.3$ cm
- $R_0 = 0.1588$ cm
- $\frac{dP}{dz} = 206844000$ g(cm)$^{-1}$(s)$^{-2}$

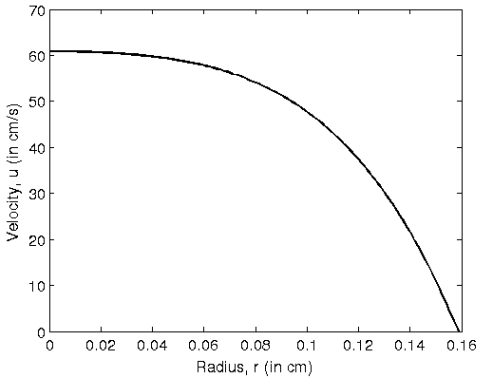

Figure 3: Fully developed velocity distribution for Lucite

2.2 Temperature distribution in the fully developed region

In Wei and Luo (2003), it is shown that for large z, i.e, at the position far from the entrance the temperature distribution stabilizes. In this case, $\frac{\partial T}{\partial z} = 0$, and (3) reduces to

$$k\left(\frac{\partial^2 T}{\partial r^2} + \frac{1}{r}\frac{\partial T}{\partial r}\right) + \tau\frac{du}{dr} = 0.$$

Substitution of (1) to the above equation yields

$$\kappa\left(\frac{\partial^2 T}{\partial r^2} + \frac{1}{r}\frac{\partial T}{\partial r}\right) - \eta\left(\frac{du}{dr}\right)^2 = 0. \tag{7}$$

Next, we use the relation $-\frac{du}{dr} = \frac{1}{\eta}$ as proposed by Gee and Lyon(1956) to get

$$\kappa\left(\frac{\partial^2 T}{\partial r^2} + \frac{1}{r}\frac{\partial T}{\partial r}\right) - \frac{1}{\eta} = 0,$$

where $\frac{1}{\eta} = \frac{1}{\eta_0}(1 + k\tau^2)$, $\eta_0 = Ae^{\gamma/T}$, with A and γ material dependent constants. If the temperature of the wall is set to be the same as the temperature of the fluid at the entrance, we can assume that η_0 is independent of T and hence we can fixe T to be equal to the wall temperature T_w. Equation (7) can now be written as

$$\frac{\partial^2 T}{\partial r^2} + \frac{1}{r}\frac{\partial T}{\partial r} = \alpha + \beta r^2,$$

where

$$\alpha = \frac{1}{\kappa A e^{\gamma/T_w}} \quad \text{and} \quad \beta = \frac{k}{4\kappa L_0^2 A e^{\gamma/T_w}} \left(\frac{dP}{dz}\right)^2.$$

The general solution of the above equation is given by

$$T(r) = C_1 \ln(r) + C_2 + \frac{1}{4}\alpha r^2 + \frac{1}{16}\beta r^4, \quad r > 0.$$

The temperature profile obtained from this solution is shown is Figure 4 (a) with parameters as used in Section 2.1 (for Lucite) and with $T_w = 525.15$ K, $A = 6.3 \times 10^{-13}$ poise, and $\gamma = 19500$ K.

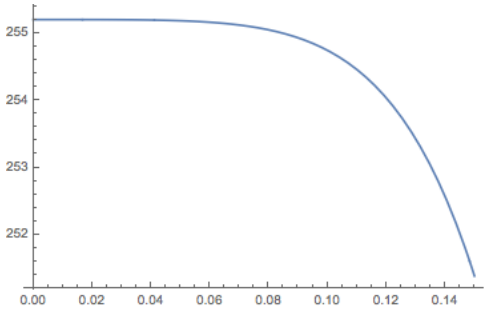

(a) Computed Temperature

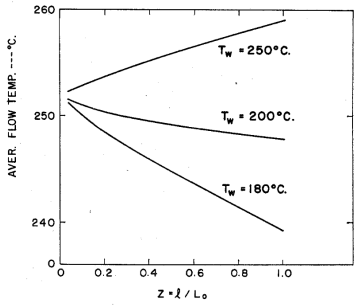

(b) Temperature by experiment

Figure 4: Steady-state Temperature distribution

Figure (4) compares the computed temperature and the measured temperature, based on the experimental data of Gee and Lyon(1956). Note that Figure (4a) shows average temperature, which can be found as a point on the line form the Figure (4b). It can be seen that our semi-analytic solution represents the experimental solution rather closely. This solution will be used in the following section on using the Galerkin finite element procedure for computation of the temperature distribution in the tube.

3 Finite Element Approximation of Temperature Distribution

In this section we derive a finite element approximation to (3). To obtain such an approximation we shall start with the heat equation in the Cartesian coordinate

$$\rho C_p u \frac{\partial T}{\partial z} = \kappa\left(\frac{\partial^2 T}{\partial x^2} + \frac{\partial^2 T}{\partial y^2} + \frac{\partial^2 T}{\partial z^2}\right) + f, \quad \text{in } \Omega \subset R^3, \tag{8}$$

where $f = f(x, y, z)$ is a source term, with the boundary conditions

$$\begin{aligned} T &= T_1 \qquad\qquad \text{on} \quad C_1, \\ -\kappa \frac{\partial T}{\partial n} &= \beta(T - T_2) \qquad \text{on} \quad C_2, \end{aligned} \tag{9}$$

with $C_1 \cup C_2 = \partial\Omega$, $C_1 \cap C_2 = \emptyset$. Here, T_1 and T_2 are temperatures on C_1 and C_2, respectively, β the heat transfer coefficient, and n the outer normal component to C_2.

Let w be a test function. Multiplying both sides of (8) by w and inte-

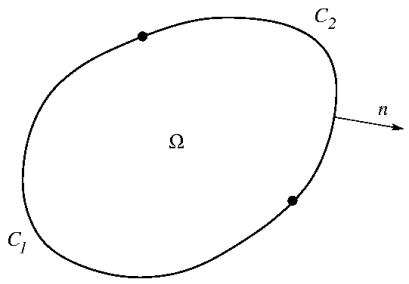

Figure 5: Computational domain

grating over Ω yields

$$\int_\Omega \rho C_p u \frac{\partial T}{\partial z} w d\Omega = \int_\Omega \left(\kappa \nabla^2 T + f\right) w d\Omega,$$

the so-called weak formulation of (8), with $\nabla^2 T = \frac{\partial^2 T}{\partial x^2} + \frac{\partial^2 T}{\partial y^2} + \frac{\partial^2 T}{\partial z^2}$. By applying integration by parts, we get

$$\begin{aligned} &\int_\Omega \rho C_p u \frac{\partial T}{\partial z} w d\Omega + \int_\Omega \kappa \nabla T \cdot \nabla w d\Omega \\ &= \int_{\partial\Omega} \kappa \nabla T \cdot \mathbf{n} w dS + \int_\Omega f w d\Omega. \end{aligned}$$

which, after imposing (9), can be written as:

$$\begin{aligned} \int_\Omega \left(\rho C_p u \frac{\partial T}{\partial z} + \kappa \nabla T \cdot \nabla w\right) dV &= \int_\Omega f w d\Omega + \int_{\partial\Omega} \kappa \nabla T \cdot \mathbf{n} w dS \\ &= \int_\Omega f w d\Omega + \int_{C_1} \kappa \nabla T \cdot \mathbf{n} w dS + \int_{C_2} \beta(T - T_2) w dS. \end{aligned}$$

Consider a point $P(x, y, z) \in \Omega$. This point in the Polar coordinate has the coordinate (r, θ, z) satisfying the relation

$$\begin{bmatrix} x \\ y \\ z \end{bmatrix} = \begin{bmatrix} r\cos(\theta) \\ r\sin(\theta) \\ z \end{bmatrix}.$$

Then

$$\begin{bmatrix} \frac{\partial T}{\partial r} \\ \\ \frac{\partial T}{\partial \theta} \\ \\ \frac{\partial T}{\partial z} \end{bmatrix} = \begin{bmatrix} \cos\theta & \sin\theta & 0 \\ -r\sin\theta & r\cos\theta & 0 \\ 0 & 0 & 1 \end{bmatrix} \begin{bmatrix} \frac{\partial T}{\partial x} \\ \\ \frac{\partial T}{\partial y} \\ \\ \frac{\partial T}{\partial z} \end{bmatrix}.$$

For an axisymmetric problem, T is constant along the angular direction, so $\frac{\partial T}{\partial \theta} = 0$. We have, therefore,

$$\nabla T := \begin{bmatrix} \frac{\partial T}{\partial x} \\ \\ \frac{\partial T}{\partial y} \\ \\ \frac{\partial T}{\partial z} \end{bmatrix} = \begin{bmatrix} \cos\theta & 0 \\ \sin\theta & 0 \\ 0 & 1 \end{bmatrix} \begin{bmatrix} \frac{\partial T}{\partial r} \\ \\ \frac{\partial T}{\partial z} \end{bmatrix}.$$

Similarly, for w under the axisymmetric assumption,

$$\nabla w := \begin{bmatrix} \frac{\partial w}{\partial x} \\ \\ \frac{\partial w}{\partial y} \\ \\ \frac{\partial w}{\partial z} \end{bmatrix} = \begin{bmatrix} \cos\theta & 0 \\ \sin\theta & 0 \\ 0 & 1 \end{bmatrix} \begin{bmatrix} \frac{\partial w}{\partial r} \\ \\ \frac{\partial w}{\partial z} \end{bmatrix}.$$

Thus,

$$\nabla T \cdot \nabla w = \frac{\partial T}{\partial r}\frac{\partial w}{\partial r} + \frac{\partial T}{\partial z}\frac{\partial w}{\partial z}.$$

Finally we get:

$$\int_\Omega \big(\rho C_p u \frac{\partial T}{\partial z} w + \kappa\big(\frac{\partial T}{\partial r}\frac{\partial w}{\partial r} + \frac{\partial T}{\partial z}\frac{\partial w}{\partial z}\big)\big) r dr dz + \int_{D_2} \beta T w r ds =$$

$$\int_\Omega f w r dr dz + \int_{D_1} \kappa \nabla T \cdot \mathbf{n} w r ds + \int_{D_2} \beta T w r ds.$$

Galerkin's finite element method is based on the above integral equation. In this method, we seek for an approximation to the unknown T based on a linear combination of piecewisely continuous polynomials in the domain Ω, which is divided into finite element-disjoint subdomains. For simplicity, in this work, we use the standard axisymmetric linear triangular elements as, e.g., presented in (Kythe and Wei, 2004). Let the domain Ω be partitioned into N equal triangles (see Figure 6), and define each triangular subdomain by $\Omega^{(e)}, \quad e = 1, 2, ..., N$. Consider the triangular subdomain $\Omega^{(e)}$ with three nodes i, j, k (see Figure 7). On $\Omega^{(e)}$ the test function w is approximated by the finite element shape functions $\varphi^{(e)} = [\varphi_i^{(e)} \quad \varphi_j^{(e)} \quad \varphi_k^{(e)}]$, and similarly for T by $T^{(e)} = (\varphi^{(e)})^T \begin{bmatrix} T_i^{(e)} \\ T_j^{(e)} \\ T_k^{(e)} \end{bmatrix}$ in each subdomain.

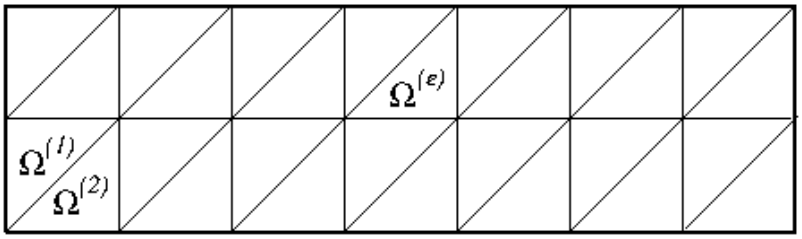

Figure 6: Partitioned domain

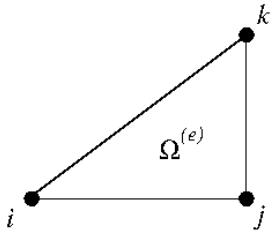

Figure 7: Partitioned domain

In particular, we use the linear shape functions

$$\begin{aligned}\varphi_i^{(e)} &= a_i^{(e)} + b_i^{(e)} r + c_i^{(e)} z \\ \varphi_j^{(e)} &= a_j^{(e)} + b_j^{(e)} r + c_j^{(e)} z \\ \varphi_k^{(e)} &= a_k^{(e)} + b_k^{(e)} r + c_k^{(e)} z\end{aligned} \tag{10}$$

where

$$\begin{aligned}[a_i^{(e)} a_j^{(e)} a_k^{(e)}] &= \frac{1}{2|\Omega^{(e)}|}[r_j^{(e)} z_k^{(e)} - r_k^{(e)} z_j^{(e)}, r_k^{(e)} z_i^{(e)} - r_i^{(e)} z_k^{(e)}, r_i^{(e)} z_j^{(e)} - r_j^{(e)} z_i^{(e)}] \\ [b_i^{(e)} b_j^{(e)} b_k^{(e)}] &= \frac{1}{2|\Omega^{(e)}|}[z_j^{(e)} - z_k^{(e)}, z_k^{(e)} - z_i^{(e)}, z_i^{(e)} - z_j^{(e)}] \\ [c_i^{(e)} c_j^{(e)} c_k^{(e)}] &= \frac{1}{2|\Omega^{(e)}|}[r_k^{(e)} - r_j^{(e)}, r_i^{(e)} - z_k^{(e)}, r_j^{(e)} - r_i^{(e)}],\end{aligned} \tag{11}$$

where $|\Omega^{(e)}|$ is the area of the triangle $\Omega^{(e)}$.

In $\Omega^{(e)}$, for the first term on LHS of (10), we have

$$\int_{\Omega^e} \rho c u \frac{\partial \varphi^{(e)}}{\partial z} (\varphi^{(e)})^T r dr dz = \frac{\rho c u |\Omega^{(e)}|}{12} \times$$
$$\begin{bmatrix} c_i^{(e)}\big(2r_i^{(e)} + r_j^{(e)} + r_k^{(e)}\big) & c_i^{(e)}\big(r_i^{(e)} + 2r_j^{(e)} + r_k^{(e)}\big) & c_i^{(e)}\big(r_i^{(e)} + r_j^{(e)} + 2r_k^{(e)}\big) \\ c_j^{(e)}\big(2r_i^{(e)} + r_j^{(e)} + r_k^{(e)}\big) & c_j^{(e)}\big(r_i^{(e)} + 2r_j^{(e)} + r_k^{(e)}\big) & c_j^{(e)}\big(r_i^{(e)} + r_j^{(e)} + 2r_k^{(e)}\big) \\ c_k^{(e)}\big(2r_i^{(e)} + r_j^{(e)} + r_k^{(e)}\big) & c_k^{(e)}\big(r_i^{(e)} + 2r_j^{(e)} + r_k^{(e)}\big) & c_i^{(e)}\big(r_k^{(e)} + r_j^{(e)} + 2r_k^{(e)}\big) \end{bmatrix} =: M^{(e)},$$

for the second term of LHS,

$$\int_{\Omega^e} \kappa \Big(\frac{\partial \varphi^{(e)}}{\partial r} \frac{\partial (\varphi^{(e)})^T}{\partial r} + \frac{\partial \varphi^{(e)}}{\partial z} \frac{\partial (\varphi^{(e)})^T}{\partial z} \Big) r dr dz = \bar{r}^{(e)} \kappa |\Omega^{(e)}| \times$$
$$\left(\begin{bmatrix} (b_i^{(e)})^2 & b_i^{(e)} b_j^{(e)} & b_i^{(e)} b_k^{(e)} \\ b_i^{(e)} b_j^{(e)} & (b_j^{(e)})^2 & b_j^{(e)} b_k^{(e)} \\ b_i^{(e)} b_k^{(e)} & b_j^{(e)} b_k^{(e)} & (b_k^{(e)})^2 \end{bmatrix} + \begin{bmatrix} (c_i^{(e)})^2 & c_i^{(e)} c_j^{(e)} & c_i^{(e)} c_k^{(e)} \\ c_i^{(e)} c_j^{(e)} & (c_j^{(e)})^2 & c_j^{(e)} c_k^{(e)} \\ c_i^{(e)} c_k^{(e)} & c_j^{(e)} c_k^{(e)} & (c_k^{(e)})^2 \end{bmatrix} \right) =: K^{(e)},$$

and for the first term on the RHS of (10)

$$\int_{\Omega^{(e)}} \varphi^{(e)} f r dr dz = \frac{f^{(e)} |\Omega^{(e)}|}{12} \begin{bmatrix} 2r_i^{(e)} + r_j^{(e)} + r_k^{(e)} \\ r_i^{(e)} + 2r_j^{(e)} + r_k^{(e)} \\ r_i^{(e)} + r_j^{(e)} + 2r_k^{(e)} \end{bmatrix} =: F^{(e)}.$$

4 Numerical result

In this section we present numerical result using the approach discussed in section 3. We compute the temperature distribution at the entrance ($z = 0$). For our finite element approximation we use two triangles, denoted by $\Omega^{(1)}$ and $\Omega^{(2)}$, to cover part of the tube near the entrance; see Figure 8. We impose the following boundary conditions: $T_w = 250°$ C and $T_0 = 252°$ C. This means that the temperature at the (global) node 1 is 252° C, or $T_1 = 252$, and so $T_3 = 250$ and $T_4 = 250$. We are seeking for the solution at the (global) node 2. For this computations we use the property of Lucite and experimental setting as described in section 2.

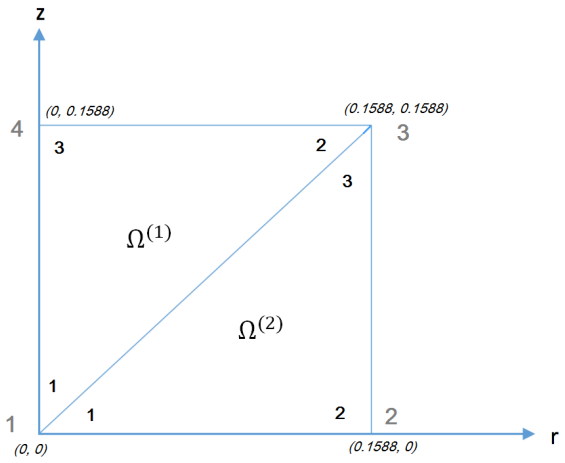

Figure 8: Illustration of local and global nodes

For the triangle $\Omega^{(1)}$, $(r_1^{(1)}, z_1^{(1)}) = (0, 0), (r_2^{(1)}, z_2^{(1)}) = (0.1588, 0.1588), (r_3^{(1)}, z_3^{(1)}) = (0, 0.1588)$. Furthermore,

$$
\begin{aligned}
[a_1^{(1)} a_2^{(1)} a_3^{(1)}] &= [1 \quad 0 \quad 0], \\
[b_1^{(1)} b_2^{(1)} b_3^{(1)}] &= [0 \quad 6.2972 \quad -6.2972], \\
[c_1^{(1)} c_2^{(1)} c_3^{(1)}] &= [-6.2972 \quad 0 \quad 6.2972].
\end{aligned}
$$

We have the local matrices, with $u(\bar{r}^{(1)}) = 58.642$, $u(\bar{r}^{(2)}) = 45.141$, $f^{(1)} = \tau \times \frac{du}{d\bar{r}^{(1)}} = -56260024.35$, and $|\Omega^{(1)}| = 0.0126$,

$$M^{(1)} = 98.729 \begin{bmatrix} -6.2972(0.1588) & -6.2972(0.3176) & -6.2972(0.1588) \\ 0(0.1588) & 0(0.3176) & 0(0.1588) \\ 6.2972(0.1588) & 6.2972(0.3176) & 6.2972(0.1588) \end{bmatrix}$$
$$= \begin{bmatrix} -98.729 & -197.458 & -98.729 \\ 0 & 0 & 0 \\ 98.729 & 197.458 & 98.729 \end{bmatrix},$$

$$K^{(1)} = 0.0529 \times 0.00205 \times 0.0126 \begin{bmatrix} (6.2972)^2 & 0 & -(6.2972)^2 \\ 0 & (6.2972)^2 & -(6.2972)^2 \\ -(6.2972)^2 & -(6.2972)^2 & 2(6.2972)^2 \end{bmatrix},$$

and

$$F^{(1)} = \frac{f^{(1)}|\Omega^{(1)}|}{12} \begin{bmatrix} 2r_1^{(1)} + r_2^{(1)} + r_3^{(1)} \\ r_1^{(1)} + 2r_2^{(1)} + r_3^{(1)} \\ r_1^{(1)} + r_2^{(1)} + 2r_3^{(1)} \end{bmatrix} = \begin{bmatrix} -9387.289 \\ -18774.577 \\ -9387.289 \end{bmatrix}.$$

For the triangle $\Omega^{(2)}$, $(r_1^{(2)}, z_1^{(2)}) = (0, 0)$, $(r_2^{(2)}, z_2^{(2)}) = (0.1588, 0)$, $(r_3^{(2)}, z_3^{(2)}) = (0.1588, 0.1588)$, and

$$[a_1^{(2)} a_2^{(2)} a_3^{(2)}] = [1 \quad 0 \quad 0],$$
$$[b_1^{(2)} b_2^{(2)} b_3^{(2)}] = [-6.2972 \quad 6.2972 \quad 0],$$
$$[c_1^{(2)} c_2^{(2)} c_3^{(2)}] = [0 \quad -6.2972 \quad 6.2972].$$

We have the local matrices, with $u(\bar{r}^{(2)}) = 45.141$, $f^{(2)} = \tau \times \frac{du}{d\bar{r}^{(1)}} = -497915380$, and $|\Omega^{(2)}| = 0.0126$,

$$M^{(2)} = 76 \begin{bmatrix} 0(0.3176) & 0(0.4764) & 0(0.4764) \\ -6.2972(0.3176) & -6.2972(0.4764) & -6.2972(0.4764) \\ 6.2972(0.3176) & 6.2972(0.4764) & 6.2972(0.4764) \end{bmatrix}$$
$$= \begin{bmatrix} 0 & 0 & 0 \\ -152 & -228 & -228 \\ 152 & 228 & 228 \end{bmatrix},$$

$$K^{(2)} = 0.1059 \times 0.00205 \times 0.0126 \begin{bmatrix} (6.2972)^2 & -(6.2972)^2 & 0 \\ -(6.2972)^2 & 2(6.2972)^2 & -(6.2972)^2 \\ 0 & -(6.2972)^2 & (6.2972)^2 \end{bmatrix},$$

and

$$F^{(2)} = \frac{f^{(2)}|\Omega^{(2)}|}{12}\begin{bmatrix} 2r_1^{(2)} + r_2^{(2)} + r_3^{(2)} \\ r_1^{(2)} + 2r_2^{(2)} + r_3^{(2)} \\ r_1^{(2)} + r_2^{(2)} + 2r_3^{(2)} \end{bmatrix} = \begin{bmatrix} -166159.735 \\ -249239.602 \\ -249239.602 \end{bmatrix}.$$

Let $K^{(e)} = [K_{i,j}^{(e)}]_{i,j=1,2,3}$ and similarly for $M^{(e)}$, and $F^{(e)} = [F_i^{(e)}]_{i=1,2,3}$. The global matrices associated with the $\Omega^{(1)}$ and $\Omega^{(2)}$ are

$$\begin{aligned} M &= \begin{bmatrix} M_{11}^{(1)} + M_{11}^{(2)} & M_{12}^{(2)} & M_{12}^{(1)} + M_{13}^{(2)} & M_{13}^{(1)} \\ M_{21}^{(2)} & M_{22}^{(2)} & M_{23}^{(2)} & 0 \\ M_{21}^{(1)} + M_{31}^{(2)} & M_{32}^{(2)} & M_{22}^{(1)} + M_{33}^{(2)} & M_{23}^{(1)} \\ M_{31}^{(1)} & 0 & M_{32}^{(1)} & M_{33}^{(1)} \end{bmatrix} \\ &= \begin{bmatrix} -98.7 & 0 & -197.4 & -98.7 \\ -152 & -228 & -228 & 0 \\ 152 & 228 & 228 & 0 \\ 98.7 & 0 & 197.4 & 98.7 \end{bmatrix}, \end{aligned}$$

and

$$\begin{aligned} K &= \begin{bmatrix} K_{11}^{(1)} + K_{11}^{(2)} & K_{12}^{(2)} & K_{12}^{(1)} + K_{13}^{(2)} & K_{13}^{(1)} \\ K_{21}^{(2)} & K_{22}^{(2)} & K_{23}^{(2)} & 0 \\ K_{21}^{(1)} + K_{31}^{(2)} & K_{32}^{(2)} & K_{22}^{(1)} + K_{33}^{(2)} & K_{23}^{(1)} \\ K_{31}^{(1)} & 0 & K_{32}^{(1)} & K_{33}^{(1)} \end{bmatrix} \\ &= 10^{-4}\begin{bmatrix} 1.6277 & -1.0851 & 0 & -0.5426 \\ -1.0851 & 2.1702 & -1.0851 & 0 \\ 0 & -1.0851 & 1.6277 & -0.5426 \\ -0.5426 & 0 & -0.5426 & 1.0851 \end{bmatrix}. \end{aligned}$$

Furthermore,

$$F = \begin{bmatrix} F_1^{(1)} + F_1^{(2)} \\ F_2^{(2)} \\ F_2^{(1)} + F_3^{(2)} \\ F_3^{(1)} \end{bmatrix} = \begin{bmatrix} -175547.024 \\ -249239.602 \\ -268014.179 \\ -9387.289 \end{bmatrix}$$

and

$$Q = \begin{bmatrix} Q_1 \\ 0 \\ Q_3 \\ Q_4 \end{bmatrix}.$$

Let $\mathbf{T} = [T_1 \quad T_2 \quad T_3 \quad T_4]^T$. The finite element approximation to the solution is then given by the solution of the system of equations

$$(M + K)\mathbf{T} = F + Q. \tag{12}$$

In our case the system reads

$$\left(\begin{bmatrix} -98.7 & 0 & -197.4 & -98.7 \\ -152 & -228 & -228 & 0 \\ 152 & 228 & 228 & 0 \\ 98.7 & 0 & 197.4 & 98.7 \end{bmatrix} + 10^{-4} \begin{bmatrix} 1.6277 & -1.0851 & 0 & -0.5426 \\ -1.0851 & 2.1702 & -1.0851 & 0 \\ 0 & -1.0851 & 1.6277 & -0.5426 \\ -0.5426 & 0 & -0.5426 & 1.0851 \end{bmatrix} \right)$$
$$\times \begin{bmatrix} 252 \\ T_2 \\ 250 \\ 250 \end{bmatrix} = \begin{bmatrix} -175547.024 \\ -249239.602 \\ -268014.179 \\ -9387.289 \end{bmatrix} \begin{bmatrix} Q_1 \\ 0 \\ Q_3 \\ Q_4 \end{bmatrix}$$

Observe that the entries in the K matrix are small compared to the entries of M and can be neglected. This is consistent with the intuition that in the entrance region, convective heat transfer dominates conductive heat transfer. T_2 can then be computed by using only the second equation in the above system, which gives $T_2 = 675$. Figure 9 (a) below gives temperature profile of the Lucite which was taken from Lucite Diakon Technical Manual (lucitediakon.com), which is obtained experimentally. This compares favorably with our result.

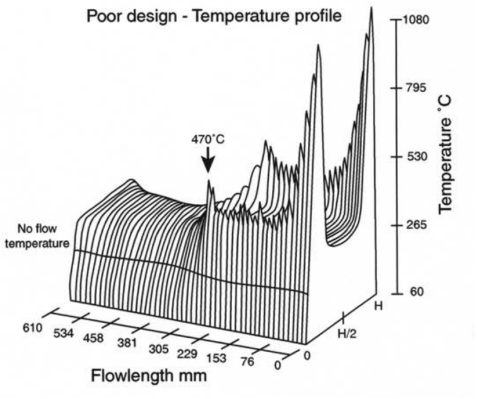

(a) lucitediakon.com

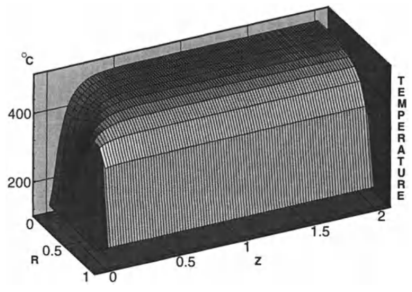

(b) Wei & Luo, 2003

Figure 9: Pictures of Temperature in the entrance to the tube

By using finite element method even for non-constant temperature we can divide our tube in hundreds of tiny triangles and find temperature at any point and obtain a temperature profile similar to the one shown in Figure 9 (b). Also, it is very important to find entrance velocity and construct entrance temperature profile. The future aim of this work is to solve the following equation, which describes entrance temperature behavior:

$$\rho C \frac{\partial T}{\partial z} = \nabla \cdot (\kappa \nabla T) + \eta \big(\frac{du}{dr}\big)^2 \tag{13}$$

where η is a viscosity function, and the last term in the equation results from Arrhenius Law as the heat source from shear strain of the fluid flow.

5 Conclusion

The behavior of the temperature for lucite was shown in this work. First, we construct velocity profile for fully developed region. After that temperature for fully developed region was found. Finally, entrance temperature was found at given point. We can assume that our result is true, because in every step we compare our solution with result from literature.

6 Acknowledgement

I would like to express my gratitude to all my Professors, specially to Professor Dongming Wei, Professor Yogi Erlangga and Professor Kira Adaricheva for their help and support during my bachelor years. Also, I am very grateful to my friends Nursultan Svankulov, Nurbek Tazhimbetov, Zhuldyzay Baki and Alina Iskakova. Thanks to my mom!

References

1. Agur, E.E. Vlachopoulos, J. (1981). Heat transfer to molten polymer flow in tubes. *Journal of Applied Polymer Science*, 26(3), 765-773.

2. Gee, R.E Lyon, J.B. (1957). Non isothermal flow of viscous non-Newtonian fluids. *Fluid mechanics in chemical engineering* , 49(6), 956-960.

3. Innovativecontrolscom. (2016). *Innovativecontrolscom.* Retrieved 9 May, 2016, from http://innovativecontrols.com/sites/default/files/images /Figure201.jpg.

4. Lucitediakoncom. (2016). Lucitediakoncom. Retrieved 9 May, 2016, from http://lucitediakon.com/wp-content/uploads/2014/08/Lucite-Diakon-Technical-Manual.pdf

5. Wei, D. Zhang, Z. (2001). Decay estimates of heat transfer to melton polymer flow in pipes with viscous dissipation. *Electronic Journal of Differential Equations*, 2001(39), 1-14.

6. Wei, D. Luo, H. (2003). Finite element solutions of heat transfer in molten polymer flow in tubes with viscous dissipation. *International Journal of Heat and Mass Transfer*, 46(16), 3097-3108.

7. Wei, D. Kythe, P.K. (2004). *An Introduction to Linear and Nonlinear Finite Element Analysis.* (1st ed.). New-York: Springer Science+Business Media.